Applied Science and Engineering Progress, Vol. 20, No.2, 2027, 8220

Research Article

Thermo-mechanical Creep Performance of Kevlar and Woven Glass Fiber-based Composites Through Experimental Techniques and Viscoelastic Modelling

T.P. Sathishkumar*
Material Research Center, Department of Mechanical Engineering, Kongu Engineering College, Erode, Tamil Nadu, India.

L. Rajeshkumar**
CoE – Advanced Materials Synthesis and Department of Mechanical Engineering, Alliance School of Applied Engineering, Alliance University, Bangalore, Karnataka, India

S. Sivalingam
Department of Mechanical Engineering, JJ College of Engineering and Technology, Tiruchirapalli, Tamil Nadu, India

R. Gopinath
Department of Civil Engineering, University College of Engineering Tindivanam, Melpakkam, Tindivanam, Tamil Nadu, India

M. Sathishkumar***
Department of Mechanical Engineering, Amrita School of Engineering, Amrita Vishwa Vidyapeetham, Chennai, India

Corresponding Authors: *tpsathish81@gmail.com, **lrkln27@gmail.com, *** m_sathishkumar@ch.amrita.edu
DOI: 10.14416/j.asep.2026.08.003
Received: 16 March 2026; Revised: 11 April 2026; Accepted: 8 May 2026; Published online: 10 August 2026

Abstract

Fiber-reinforced composites play a significant role in various temperature-dependent engineering applications. Hybrid composites, incorporating reinforcements such as glass, carbon, and Kevlar fibers, significantly improve the mechanical properties of polymer composites. The present work aims to study the thermo-mechanical creep behaviour of Kevlar- and woven glass-fiber-reinforced epoxy hybrid (KGFRH) composites through experimental testing and viscoelastic modelling. The composites were fabricated using a compression moulding process. The tensile creep behaviour of the hybrid composites was investigated by varying the applied loads to 50, 75, and 100 kg and the temperatures to 100, 120, and 140°C. The creep strain versus time data were recorded for all samples. The creep strain gradually increased with increasing load and temperature. At lower load and temperature conditions, the creep curve showed better performance because all three stages of creep failure were observed, whereas at higher load and temperature conditions, only the primary and secondary stages were noted. The combination of a 50 kg load and 100°C temperature showed the best results. Viscoelastic numerical models, including Burger's model and the Norton model, were used to predict the elastic modulus, coefficients, and curve-fitting values. Kevlar/glass–epoxy composites with improved thermo-mechanical behaviour can be utilized in lightweight and protective applications.

Keywords: Creep behaviours, Hybrid fiber composites, Lightweight fiber, Numerical modelling, Tensile properties

1 Introduction

Currently, fiber-reinforced polymer composites (FRP) are widely used for various structural applications in various environmental conditions. These are developed by considering various matrix types, fiber treatments, processing techniques, etc. Followed by studying the various mechanical, thermal, dynamic, and vibration characteristics that are sustainable and future modelling for advanced engineering applications [1]. Creep behaviours of the FRP have shown the life of the material under constant stress over the period and viscoelastic behaviours were evaluated at higher temperatures [2]. The *Cocos* *nucifera* (CN) fiber materials have better mechanical stability than the *Canarium schweinfurthii* (CS) materials. The creep coefficient was continuously increased by increasing the working temperature; the CN fiber materials showed a higher creep coefficient than the CS [3]. The isothermal creep behavior of glass fiber/epoxy and graphene oxide with glass fiber/epoxy composites was conducted between 30°C and 120°C. It showed that the long-term durability of the composites slowly dropped by increasing the isothermal temperature, which caused quick viscoelastic behaviors of the composites [4], [5]. The working temperature of the E-glass epoxy composites directly influences the creep compliance. Increasing the temperature and applied stress increased the creep compliance [6-8]. The three-point flexural creep behaviors of glass-carbon FRP were recorded for 5000 hours under 50, 60, and 70% ultimate load, and the testing temperature ranged from -20°C to 20°C. The creep deflection was gradually increased by increasing the ultimate load, and a higher deflection was found for freeze-thaw samples than for the untreated sample [9].

The higher bonding between fiber and matrix present in the carbon FRP has lower creep rates compared with the glass FRP, and also, non-bonding interaction was found to be less between the fiber and matrix [10]. Comparing the carbon PEEK and carbon epoxy composites, the creep strain was found to be higher for PEEK composites at all stress conditions because they withstand longer times to deform and also have better bonding between the carbon fiber and PEEK. Increasing the testing temperature lowered the strain rate and time taken for creep failure [11]. The void content present at the interface of the glass fiber and epoxy decreased the modulus in the glassy region, and creep deformation was found to be higher [12]. Tensile creep behaviors of short carbon fiber polyetherimide composites have better creep resistance by increasing the fiber content. The superposition principle was adopted to predict the long-term creep analysis [13], [14]. The creep deformation increased quickly when testing temperatures exceeded the glass transition point because viscoelastic behaviors became easier. Material creep received restraint from fiber reinforcement, although inadequate bond strength between reinforcement fibers and matrix [15]. The creep strain was linearly increased with logarithmic time at higher stress, but the creep strain gradually declined with increasing testing time. The creep parameters were obtained from the power law model, and the predicted creep deformation was not affected at any stress level [16].

The unidirectional carbon fiber lamina had shown lower strain failures at higher loading stress conditions. The power law method estimated the overall higher creep strain, which predicted the total creep strains [17]. The creep behaviors of glass FRP were studied at 25, 60, and 80°C, which showed that negligible creep behaviors were obtained at lower temperatures, but it was found to be higher at elevated temperatures [18]. The creep strain was recorded considering three load levels that were applied to the balau wood and pultruded glass FRP composites. The stable strain curve was observed for the GFRP composite more than wood, which had only the primary and secondary stages of the creep curve. The Burger, Findley, and Norton simplified models were used to predict the viscoelastic behaviours and the modulus [19], [20]. The typical three-stage creep deformation behaviours did not show over the life due to varying the fiber diameter over the composites along unidirectional [21]. The 3D printed nylon, nylon glass, nylon Kevlar and nylon carbon fiber composites had shown a lower creep rate in nylon carbon fiber than others and compared to higher temperatures, the creep rate was found to be higher at room temperature [22].

The fiber content played an important role in the creep behaviours of basalt FRP bars. The bar diameter of 6 mm with higher fiber content have showed led creep rate than the 10 mm diameter [23]. The total strain rate was found to be lower at higher stress, and the power law model was shown good method to determine the creep strain, but it estimated the creep strain higher [24]. The Burgers and the Findely power law model were used to predict the viscoelastic behaviours of polyamide 66 nanocomposites. The Findely power law model was more adaptable for predicting the long-term creep response [25]. Recently, the synthetic fiber reinforced polymer composites have been widely used for various applications, especially in higher temperature zones. The creep behaviours are essential for synthetic composites to show better performance. Literature dealing with Kevlar/glass hybrid composites and evaluating their creep behaviour is meagre. Accordingly, the present work is to investigate the creep behaviours of hybrid fiber reinforced epoxy composites with Kevlar and glass fiber woven mat at different temperatures and different loading (stress) conditions. The selected fiber-matrix ratio (60:40 by weight) is taken for the development of the hybrid composites.

2 Materials and Methods

2.1 *Materials used*

The Kevlar and glass fiber fabrics, epoxy resin and hardener (HY951) were purchased from Covai Seenu industry, Coimbatore, Tamil Nadu and India. Table 1 shows the properties of the Kevlar and glass fibers. Figure 1a shows the woven fabrics for preparing the high-strength fiber-reinforced epoxy composite laminates. It has good adhesion with synthetic fibers, good mechanical properties, and less shrinkage compared to other thermoset resins.

Table 1: General properties of matrix and reinforcements [4], [6].

Properties	Fabrics		Resin
	Glass fiber	Kevlar fiber (K29)	
Density (g/cc)	2.54	1.44	1.16
Tensile strength (MPa)	2300 – 2400	3620 ± 68	24
Young's Modulus (GPa)	75 - 80	131 ± 8	0.5
Glass Transition temperature (Tg) (°C)	-	-	80-150

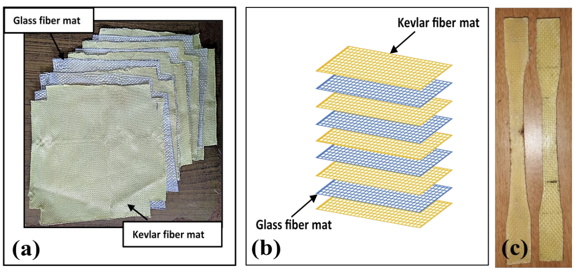

Figure 1: a) Stacking sequence, b) Glass and Kevlar fiber mat and c) Tensile creep test sample.

2.2 *Composites fabrication*

The composite was prepared by a hand lay-up process followed by a compression molding process with the help of a steel plate die. The layering patterns of the woven fabrics are shown in Figures 1a and 1b. The size of the laminas was 240 mm in length × 200 mm in width. The resin-hardener mixture in the ratio of 10:2 was prepared using a mechanical stirrer at 50 rpm for 10 minutes and the releasing agent of liquid polyvinylchloride was coated on the inside surface of the mould, which helps to easily remove the solidified composites. Before laminating, the laminas were completely dipped in resin solution and laid one-by-one in the female die. A steel roller was rolled over every layup to remove the gas formation in between the laminas and ensure the even distribution of resin over the fabric laminates. The steel mould was pressed in a hydraulic press with 25 bar pressure for 2 hours and then post-cured at 45 °C for 1 hour. The fiber volume fraction was maintained as 50 % while the resin was maintained at 50 %. The glass fiber is normally brittle nature, which can break easily when it is laminated as outer layers. To avoid this problem, the Kevlar fiber is placed in the outer layers. The number of layers is 9, which has 5-layer Kevlar and 4-layer glass fiber mats with a 60:40 weight ratio of the fibers resulting in KGFRH composites. Alternative layers of Kevlar and Glass fibers were stacked until the required 9 layers were attained and after post-curing, the composite thickness was found to be 3.4 mm.

2.3 *Tensile creep test*

The tensile creep testing samples were cut from the composite plate according to ASTM D638 (Figure 1c) and the tests were carried out in accordance to ASTM D2990 standards [13], [14]. The samples were tested in creep testing machine (Model: TEC-SOL) (Figure 2). The maximum creep loading of machine is 500 kg (5000 N) and the temperature range is from 0 °C to 300 °C. The selected three level of constant loading were 50 kg (σ_{max} =14 MPa), 75 kg (σ_{max} =21 MPa) and 100 kg (σ_{max} = 28 MPa) and varying temperature of 100 °C, 120 °C, and 140 °C respectively. The sample was loaded in the heating chamber using special fixture. The dead load was added in the right side of beam at the bottom of vertical rod (i.e. loading point). Finally, the heating chamber was closed, and the heating temperature was set through data acquisition system (DQS). The thermocouple was used to control the temperature of the chamber through Data Acquisition System (DAS), and the failure was determined by the rupture of the specimen. The plot of creep strain versus time taken was recorded using DQS and three samples were tested in each condition.

2.4 *Tensile test*

The tensile samples were cut according to ASTM D638 (Figure 1c) with dimensions of 165 mm length, 19 mm width and 3 mm thickness (gauge length of 50 mm). Tensile tests were carried out in a Universal Testing Machine (Make: DEEPAK poly plastic Pvt., and Model: DX25 kN) with a load cell of 25 kN and the tensile stress and strain were calculated from the recorded load versus elongation curve. The crosshead speed of the test was 2 mm/min, and the test was conducted at room temperature. Totally, five samples were tested, and the average values were plotted. Figure 2 shows the tensile stress versus strain curve of the hybrid composite, which has a maximum stress of 320 MPa and strain of 8.2 % (Figure 3).

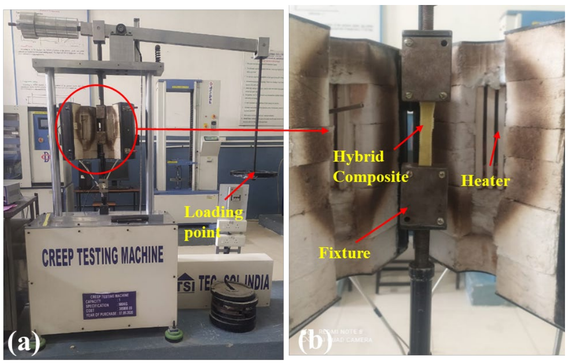

Figure 2: Creep testing machine and sample holder.

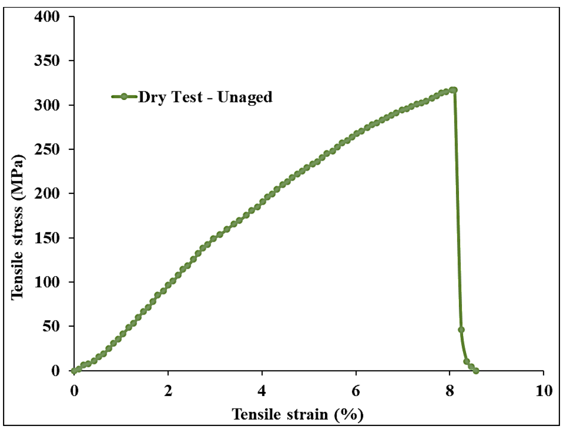

Figure 3: Average tensile stress versus tensile strain curve of the KGFRH composites.

3 Results and discussions

3.1 *Effect of temperature and load on creep behaviour*

Figure 4 shows the creep tensile curve of hybrid composites at various temperatures and loads. At 100°C, the creep curves of applied load at 50 and 75kg show the primary, secondary and tertiary zones, which closely mirror the basic creep curve. At 50kg loading, the primary zone lies between 0 and 300 hours, the secondary zone starts from 300 hours to 530 hours, and the tertiary zone starts from 530 to 701 minutes. The longer creep strain rate of 11.14% is obtained for 50 kg loading due to the slower propagation of viscoelastic deformation and this strain rate was gradually increased to higher values in the tertiary zone due to physical changes in the composites. Similarly, at 75 kg loading, the primary and secondary stages start from 0 to 210 hours and 210 hours to 401 hours. But the tertiary curve occurs very shortly between 390 and 419 hours due to increasing the applied load and the maximum creep strain rate of 7.98 % is obtained. Compared to 50 kg loading, the 75 kg loading has shown less time to creep failure and has three zones. At 100 kg loading, the primary curve starts from 0 to 231 hours and the secondary curve up to 259 hours. The tertiary curve is found from 261 to 271 hours, which is less because the higher loading time taken was reduced and from shorter viscoelastic deformation and the obtained creep strain rate was 4.44 %. Among these, the 50 kg loading at 100 °C shows the long-term secondary creep curve, which has stable and higher creep behaviour. This may be due to slow propagation of microcracks, fewer microcracks between fiber and matrix, and high resistance to fiber pull-outs. At 120°C, the growth of the curve at 50 kg loading shows primary and secondary zones, which start from 0 to 104 hours and 104 to 329 hours due to less applied load. The tertiary zone is almost absent due to temperature and the sudden formation of viscoelastic deformation. It has a maximum creep strain of 5.9 %.

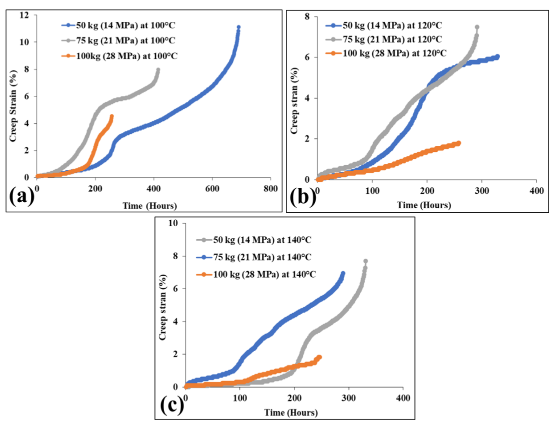

Figure 4: Creep curves of KGFRH composites at (a) 100 °C, (b) 120 °C, (c) 140 °C.

At 75 kg, the curve shows primary and tertiary zones; the elasticity changes phases from primary to tertiary. They start from 0 to 87 hours and up to 277. It has a creep strain of 7.79 %. At 100 kg, the curve shows only the primary zone because the higher load leads to faster deformation with a shorter period, 258 hours with 1.8 % creep strain. At 140 °C, the creep curve at 50 kg loading shows three zones which start from 0 to 228 hours, 228 to 321 and 321 to 331 hours. The primary zone is taken higher time to the formation of creep strain than the secondary and tertiary zones. The time taken for the tertiary zone is less. The creep strain is found 7.6 %. At 75 kg loading, the formation curve has only the primary and secondary zones. It starts from 0 to 271 and 271 to 289 hours and that has 6.9 % creep strain. At 100 kg loading, the curve shows only the primary zone, which ends at 236 hours, and the creep strain is 1.67 %. Increasing the applied loads and temperatures drastically reduced the creep strain and time taken for deformation due to faster formation of viscoelastic deformation.

The applied load or stress on the hybrid composites varies the creep behaviours. The deformation was different for different loadings at different temperatures. It can be stated that at 100 °C, which is closer to the minimal Tg of the epoxy, the creep deformation was minimal due to the stiff glassy state of the epoxy. As the temperature approached the Tg of the epoxy, stress relaxation was allowed by the polymeric chain mobility without much deformation. At higher temperatures, the polymeric chain mobility increases, thereby reducing creep stability. The elastic behaviours of the hybrid composite depend purely on applied load [17], [23]. It could be seen that all curves are taken for a higher duration for initial deformation at all loads and temperatures. However, the range of deformation is gradually reduced due to increasing the load with temperature, which means the faster viscoelastic formation.

3.2 *Creep compliance*

Figure 5 shows the time dependent creep compliance of KGFRH composites. These curves show the long-term durability of the hybrid composites. The following relation, shown in equation 1, is used to generate the creep compliance curve.

$$\text{Creep compliance (C)} = \varepsilon(t)/\sigma_c, \ (\text{GPa}^{-1}) \quad (1)$$

Where, $\varepsilon(t)$ is the strain under constant stress, σ_c is the constant applied stress (GPa)

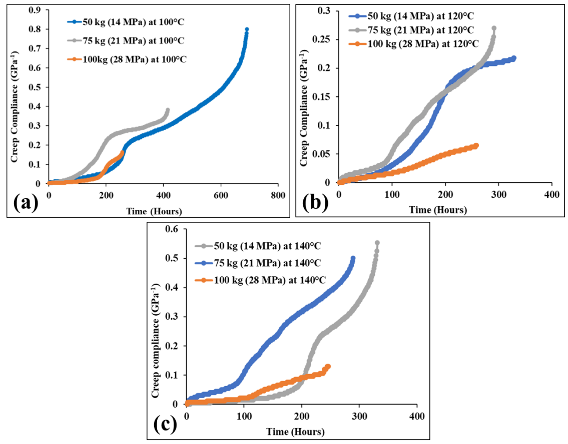

Figure 5: Creep compliance of KGFRH composites at time versus three different loading at (a) 100 °C, (b) 120 °C, (c) 140 °C.

The creep curves of all samples have stable performance in all loading and temperature conditions, and also show a steady outcome. The curves show that increasing the temperature increases the creep compliance. This trend was confirmed by Asyraf *et al.*, [19], Hoseinzadeh *et al.,* [26] and Nakai *et al.,* [27], where the higher creep compliance can be attributed to faster degradation of stability as the composite samples exposer in various temperatures. This developed the micro-cracks between the fibers and resin, also resulting in more fiber pull-outs due to increasing the applied load [28], [29-31]. In general, the 50 K loading and lower temperature possess better parameters in the development of creep rate compared to the other two loads, subsequently providing long-term behaviours for materials to withstand constant load.

3.3 *Creep numerical models*

3.3.1 Burgers model

This is the widely used model to analyse the viscoelastic behaviour of hybrid composites at various loading and temperatures. It combines the elastic and viscous elements to showcase a hybrid effect of the Maxwell and Kelvin-Voigt model, which is represented in spring, dashpot and dashpot-spring elements. These models are connected in series

Table 2: Parameters of Burgers model.

Temperature (°C)	Load (kg)/Stress (MPa)(σ)	EM (MPa)	EK (MPa)	η_m (MPa-sec)	η_K (MPa-sec)
100	50/14	73.96	3205.12	13736.26	3.50
	75/21	169.68	576.92	28846.15	8.32
	100/28	101.21	641.02	19307.65	7.91
120	50/14	54.019	2403.84	48076.92	6.00
	75/21	303.64	3505.12	54420.76	13.45
	100/28	202.42	1282.05	38461.53	11.53
140	50/14	147.92	3205.12	58076.92	8.06
	75/21	1442.9	1442.30	78896.92	14.78
	100/28	641.02	641.02	68456.92	12.08

(Figure 6). The total creep strain εB (Equation 2) is a hybrid effect of elastic strain (εM1), dashpot strain (permanent strain) (εK), and Kelvin-Voigt strain (i.e., viscoelastic strain) [29].

$$\varepsilon_B = \varepsilon_{M_1} + \varepsilon_{M_2} + \varepsilon_K \tag{2}$$

Where, the subscripts B, M, and K indicate Burgers model, Maxwell and Kelvin elements, respectively. ε denotes the strains of the Maxwell Spring, Maxwell dashpot, and Kelvin unit, respectively.

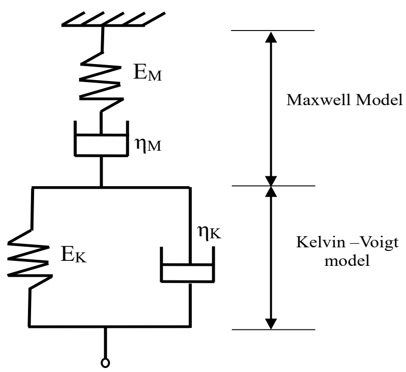

Figure 6: Linear elastic Burger model.

Considering the essential relations of the above elements and the initial conditions at t=0, the creep behaviour of the Burgers model (equation 3) can be finally obtained as follows [31].

$$\varepsilon_B = \frac{\sigma_0}{E_M} + \frac{\sigma_0}{E_k}\left(1 - exp^{\left(-\frac{E_K}{\eta_K}\right)}\right) + \frac{\sigma_0}{\eta_M}t \tag{3}$$

Where, E_M and η_M = elastic modulus and viscosity of the Maxwell spring and Maxwell dashpot, respectively; and E_k and η_k Kelvin Spring and dashpot's modulus and viscosity, respectively; and σ_0 = applied stress.

The first term denotes the instantaneous elastic deformation and is considered constant, while the second term denotes the Kelvin unit's delayed elasticity and is predominant during the early creep stage, but saturates soon after and the value would be close to σ_0/E_k. Thereafter, a linear increase in the third term during the viscous flow could be witnessed after a sufficiently long time of loading. The Burgers model, which includes the essential elements, can be applied satisfactorily to model the practical behaviours of viscoelastic materials. The elastic model (E_k and E_m) and the dynamics coefficient (η_m and η_k) are calculated from experimental data (Table 2). Elastic behaviour at the initial stage is slowly increased by increasing the applied stress, which is applicable up to 21 MPa. The maximum dynamic coefficient is obtained for the applied stress 21 MPa. It shows that the better viscoelastic behaviours occur in the hybrid composites. Further increasing the applied load (i.e. at 28 MPa) is decreasing the dynamics coefficient, which was reduced the creep strain and time, it is clearly shown in Figure 4. If the temperature increases, the similar trend is absorbed for all loads.

3.3.2 Norton's model

Norton's model is called the power law model; it is also known as the empirical model. It portrays the steady-state creep rate under different temperatures and stress. From the power law relation (Equation 4), taking log on both sides, equations 5 and 6 are obtained, and the Log(ε) versus Log(σ) is plotted based on the experimental data (Figure 7a) for different temperatures. From the graph, the coefficient of stress (n) is found to be lower with increasing temperature. At lower temperatures, the R^2 is found to be higher, which shows better results for long-term creep behaviours. The increasing temperature of the surrounding composites under creep testing is gradually decreasing the $R^{2,}$ which means that the composites deform quickly and higher temperature leads to reduced fiber-matrix bonding and increases the micro-cracks (as shown in Figure 7b). This leads to the failure of the composite.

$$\varepsilon = B\, exp^{\left(-\frac{Q}{RT}\right)}\, \sigma^{n} \tag{4}$$

$$Log(\varepsilon) = Log(B) - \left[\frac{Q}{RT}\frac{1}{2.3026}\right] + n\, log(\sigma) \tag{5}$$

$$Log(\varepsilon) = Log(B) - \frac{Q}{2303R}\frac{1000}{T} + n\, log(\sigma) \tag{6}$$

The activation energy (as shown in equations 7 and 8) is calculated from the plot shown in Figure 7.

$$Log(\varepsilon) - n\, log(\sigma) = Log(B) - \frac{Q}{2303R}\frac{1000}{T} \tag{7}$$

$$Y = Log(\varepsilon) - n\log(\sigma),\; m = -\frac{Q}{2303R},\; x = \frac{1000}{T},\; and\; C = Log(B) \tag{8}$$

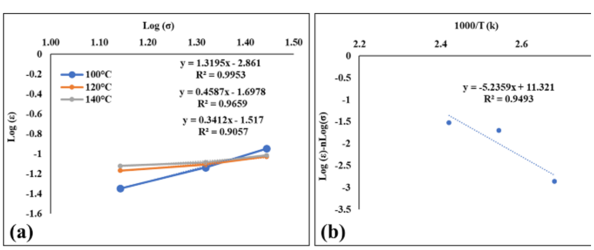

Figure 7: Activation Energy plots based on Norton's model (a) Log(ε) versus Log(σ) plot, (b) Curve fitting for the model.

3.4 *Creep service life of the hybrid composites*

The Arrhenius principle was adopted to develop Figure 8, which shows the impact of creep strain retention versus log (stress) (i.e., applied load) for all servicing temperatures. It depicts the creep strain retention of Kevlar Glass fiber mat reinforced epoxy composites. The composites were tested for creep resistance at a lower temperature of 100 °C and showed a coefficient of correlation (R2) of around 0.9834. This is more than 0.98 at 100°C; the specimen demonstrated that creep behaviour was better than the 120 and 140 °C. Even though at higher temperatures, 120 and 140 °C, the R^2 values are not below 0.90, it also gives better creep performance in the secondary zone of the curve. The creep life of the Kevlar glass fiber mat hybrid composites was estimated using x as a constant from the straight-line equation (Figure 8). The Arrhenius plot (Figure 9), which forecasts the service life of the hybrid composites, shows the percentage of creep strain retention as a function of the inverse service temperature over a 15-year period. Most of the polymer materials used in the application, manufacturers have suggested 15 years of lifetime. Therefore, estimation shows that the 1st year retention was almost 100% at 100°C, but at 120 and 140°C, has 90 and 88% retention in creep life. It is clear that increasing temperature was gradually decreasing the creep life. A creep retention of 50 % was found in the 7th year for 140°C, and in the 8th year at 120 °C. The retention for all years is uniformly reduced; it is confirmed by the value of R^2 of 0.98. Figure 10 depicts the creep strain retention of composites at various temperatures for up to 80 years. It clearly shows the creep strain retention for every year and the maximum retention was maintained at 100°C and the service life is also higher [31]–[33].

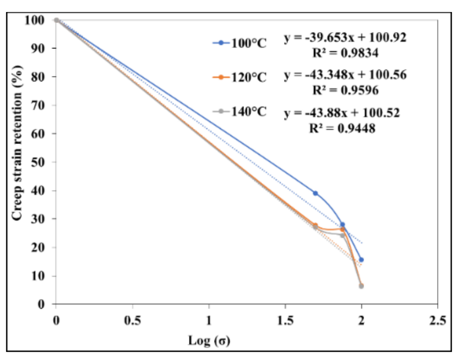

Figure 8: Creep strain retention versus log(σ).

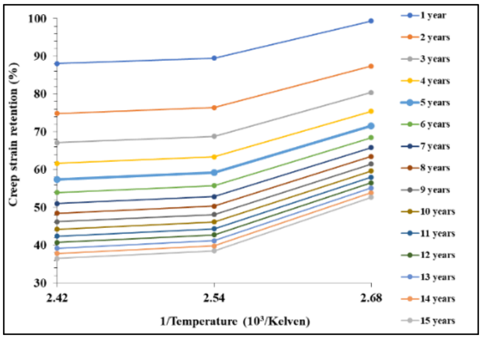

Figure 9: Creep strain retention versus temperature.

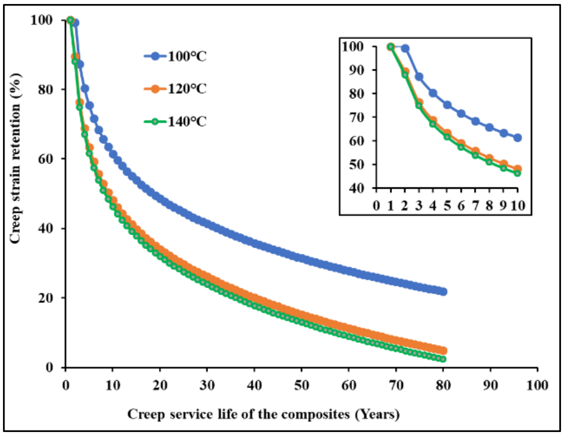

Figure 10: Creep strain versus service life of the composites.

4. Conclusions

The Kevlar- and woven glass fiber-reinforced epoxy composites were developed using a compression moulding technique, and the thermo-mechanical creep behaviour of the hybrid composites was experimentally investigated under varying loads and temperatures. This study also employed viscoelastic models, such as the Burgers and Norton–Bailey models, to predict the creep behaviour of the hybrid composites. The creep deformation was found to depend strongly on load and temperature over time. A longer steady-state creep strain was observed in the secondary creep zone for the hybrid composites tested at a load of 50 kg and a temperature of 100 °C. Moreover, this curve closely matched the reference creep curve. Similarly, the curves obtained at a load of 75 kg with 100 °C and at a load of 50 kg with 120 °C exhibited well-defined primary and secondary creep zones comparable to the reference creep curve, although the duration was shorter.

The creep compliance results demonstrated the stable performance of all samples during the creep experiments. The numerical models, namely the Burgers and Norton–Bailey models, effectively represented the viscoelastic behaviour and showed good correlation coefficients (R^2 values). In the Burgers model, the elastic modulus and dynamic coefficient were lower at lower temperatures and higher at elevated temperatures. In the Norton–Bailey model, the higher R^2 values indicated better prediction of long-term creep behaviour and creep performance. The creep life of the material was found to be higher at lower temperatures than at higher temperatures. At lower temperatures, approximately 70–80% creep strain retention was predicted over 70 years. Therefore, these materials can be effectively utilized under lower load and temperature conditions. Future work may focus on improving interfacial bonding, developing hybrid/nano-modified systems, and applying advanced predictive models to further enhance the high-temperature creep performance of epoxy–Kevlar composites.

Acknowledgments

This work has been supported by the SEED grant (Ref. No. KEC/R&D/SGRS/07/2021) sanctioned by Kongu Engineering College, Erode, India.

Author Contributions

T.P.S, L.R.K.: conceptualization, investigation, reviewing and editing; S.S, R.G, T.P.S.: investigation, methodology, writing an original draft; S.K.: research design, data analysis; L.R.K, T.P.S, M.S.K: writing—reviewing and editing, funding acquisition, project administration. All authors have read and agreed to the published version of the manuscript.

Conflicts of Interest

The authors declare no conflict of interest.

Declaration of generative AI and AI-assisted technologies in the writing process

The authors did not use any AI tools while preparing this manuscript.

References

[1] T. P. Sathishkumar, P. Navaneethakrishnan, S. Shankar, R. Rajasekar, and N. Rajini, "Characterization of natural fiber and composites–A review," *Journal of Reinforced Plastics and Composites*, vol. 32, no. 19, pp. 1457–1476, Oct. 2013, doi: 10.1177/07316844 1349532

[2] S. Wang, T. Stratford, and T. P. S. Reynolds, "Linear creep of bonded FRP-strengthened metallic structures at warm service temperatures," *Construction and Building Materials*, vol. 283, May 2021, Art. no. 122699, doi: 10.1016/j.conbuildmat.2021.122699.

[3] B. M. Ganou Koungang, D. Ndapeu, J. Tchoufang Tchuindjang, and C. A. S. Belinga, "Influence of temperature on the creep behaviour by macroindentation of *Cocos nucifera* shells and *Canarium schweinfurthii* cores (bio-shellnut wastes in Cameroon)," *Materials Research Express*, vol. 7, no. 10, Oct. 2020, Art. no. 105306, doi: 10.1088/2053-1591/abbebb.

[4] A. Anand, S. K. Ghosh, and R. K. Prusty, "Effects of seawater absorption and desorption on the long-term creep performance of graphene oxide embedded glass fiber/epoxy composites," *Polymer Composites*, vol. 41, no. 11, pp. 4861–4871, Nov. 2020, doi: 10.1002/pc.25758.

[5] K. Yorseng, R. Srisuk, V. Ayyappan, A. Thirugnanasamabandam, S. M. Rangappa, and S. Siengchin, "Lightweight Innegra–hemp/epoxy hybrid composites: Effects of weathering on mechanical, thermal, and viscoelastic properties," *International Journal of Precision Engineering and Manufacturing*, vol. 27, no. 3, pp. 1025–1041, Mar. 2026, doi: 10.1007/s12541-025-01377-5.

[6] N. Nosrati, A. Zabett, and S. Sahebian, "Long-term creep behaviour of E-glass/epoxy composite: Time-temperature superposition principle," *Plastics, Rubber and Composites*, vol. 49, no. 6, pp. 241–251, Jul. 2020, doi: 10.1080/14658011. 2020.1736867.

[7] A. Jenifer, N. Rasana, and K. Jayanarayanan, "Synergistic effect of the inclusion of glass fibers and halloysite nanotubes on the static and dynamic mechanical, thermal and flame retardant properties of polypropylene," *Materials Research Express*, vol. 5, no. 6, Jun. 2018, Art. no. 065308, doi: 10.1088/2053-1591/aac67d.

[8] L. Techawinyutham, V. Ayyappan, M. Kumar, V. Raghunathan, S. M. Rangappa, and S. Siengchin, "Sustainable epoxy composites from hemp/pineapple/glass fibers for lightweight automobile panels," *International Journal of Biological Macromolecules*, vol. 337, pt. 1, Jan. 2026, Art. no. 149392, doi: 10.1016/j.ijbiomac. 2025.149392.

[9] H. Mayookh Lal, G. Xian, S. Thomas, L. Zhang, Z. Zhang, and H. Wang, "Experimental study on the flexural creep behaviors of pultruded unidirectional carbon/glass fiber-reinforced hybrid bars," *Materials*, vol. 13, no. 4, Feb. 2020, Art. no. 976, doi: 10.3390/ma13040976.

[10] R. Qin, Y. Li, S. Y. Wong, F. Y. Teo, Z. Yu, L. Sun, and Y. Zheng, "Understanding on the creep behavior of fiber reinforced polymer via fiber/matrix interaction," *Construction and Building Materials*, vol. 451, 2024, Art. no. 138875, doi: 10.1016/j.conbuildmat.2024.138875.

[11] M. Katouzian and S. Vlase, "Creep response of carbon-fiber-reinforced composite using homogenization method," *Polymers*, vol. 13, no. 6, Mar. 2021, Art. no. 867, doi: 10.3390/polym 1306 0867.

[12] F. C. Alves, F. M. Monticeli, R. M. Neves, H. J. C. Voorwald, M. O. H. Cioffi, and H. L. Ornaghi Jr., "Influence of void content and morphology on the creep behavior on glass/epoxy composites," *Composites Communications*, vol. 25, Art. no. 100712, 2021, doi: 10.1016/j.coco. 2021.100712.

[13] Y. Y. Zhang, Z. Sun, Y. Q. Li, P. Huang, Q. Chen, and S. Y. Fu, "Tensile creep behavior of short-carbon-fiber reinforced polyetherimide composites," *Composites Part B: Engineering*, vol. 212, Art. no. 108717, 2021, doi: 10.1016/j.com positesb.2021.108717.

[14] P. S. Kumar, K. Jayanarayanan, and M. Balachandran, "Performance comparison of carbon fiber reinforced polyaryletherketone and epoxy composites: Mechanical properties, failure modes, cryo-thermal behavior, and finite element analysis," *Journal of Applied Polymer*

Science, vol. 139, no. 29, Jul. 2022, Art. no. e52494, doi: 10.1002/app.52494.

[15] S. K. Painkal, M. Balachandran, K. Jayanarayanan, N. Sridhar, and S. Kumar, "Synergistic enhancement in mechanical properties of graphene/MWCNT reinforced Polyaryletherketone–carbon fiber multi-scale composites: Experimental studies and finite element analysis," *Advanced Industrial and Engineering Polymer Research*, vol. 8, no. 1, pp. 20–36, Jan. 2025, doi: 10.1016/j.aiepr.2024.02.002.

[16] G. M. Fallatah, N. Dodds, and A. G. Gibson, "Long term creep and stress rupture of aramid fibre," *Plastics, Rubber and Composites*, vol. 36, no. 9, pp. 403–412, Nov. 2007, doi: 10.1179/174328907X248186.

[17] J. Tanks, K. Rader, S. Sharp, and T. Sakai, "Accelerated creep and creep-rupture testing of transverse unidirectional carbon/epoxy lamina based on the stepped isostress method," *Composite Structures*, vol. 159, pp. 455–462, Jan. 2017, doi: 10.1016/j.compstruct.2016.09. 096.

[18] E. Kontou, "Tensile creep behavior of unidirectional glass-fiber polymer composites," *Polymer Composites*, vol. 26, no. 3, pp. 287–292, Jun. 2005, doi: 10.1002/pc.20098.

[19] M. R. M. Asyraf, M. R. Ishak, S. M. Sapuan, and N. Yidris, "Comparison of static and long-term creep behaviors between balau wood and glass fiber reinforced polymer composite for cross-arm application," *Fibers and Polymers*, vol. 22, no. 3, pp. 793–803, Mar. 2021, doi: 10.1007/s12221-021-0512-1.

[20] N. Jain, A. Verma, and V. K. Singh, "Dynamic mechanical analysis and creep-recovery behaviour of polyvinyl alcohol based cross-linked biocomposite reinforced with basalt fiber," *Materials Research Express*, vol. 6, no. 10, Sep. 2019, Art. no. 105373, doi: 10.1088/2053-1591/ab4332.

[21] Y. Jia and B. Fiedler, "Tensile creep behaviour of unidirectional flax fibre reinforced bio-based epoxy composites," *Composites Communications*, vol. 18, pp. 5–12, Apr. 2020, doi: 10.1016/j.coco.2019.12.010.

[22] M. Mohammadizadeh, I. Fidan, M. Allen, and A. Imeri, "Creep behavior analysis of additively manufactured fiber-reinforced components," *The International Journal of Advanced Manufacturing Technology*, vol. 99, no. 5–8, pp. 1225–1234, Nov. 2018, doi: 10.1007/s00170-018-2539-z.

[23] H. Sokairge, F. Elgabbas, A. Rashad, and H. Elshafie, "Long-term creep behavior of basalt fiber reinforced polymer bars," *Construction and Building Materials*, vol. 260, Nov. 2020, Art. no. 120437, doi: 10.1016/j.conbuildmat.2020.120437.

[24] G. Bi, Z. Li, Q. Wang, and D. Jiang, "An examination of creep failure criterion based on a strain threshold identified with a power law model," *Mechanics of Time-Dependent Materials*, vol. 26, no. 1, pp. 195–209, Feb. 2022, doi: 10.1007/s11043-020-09483-9.

[25] J. L. Yang, Z. Zhang, A. K. Schlarb, and K. Friedrich, "On the characterization of tensile creep resistance of polyamide 66 nanocomposites. Part II: Modeling and prediction of long-term performance," *Polymer*, vol. 47, no. 19, Sep. 2006, pp. 6745–6758, doi: 10.1016/j.polymer.2006.07.060.

[26] F. Hoseinzadeh, S. M. Zabihzadeh, and F. Dastoorian, "Creep behavior of heat treated beech wood and the relation to its chemical structure," *Construction and Building Materials*, vol. 226, pp. 220–226, Nov. 2019, doi: 10.1016/j.conbuildmat.2019.07.181.

[27] T. Nakai, K. Toba, and H. Yamamoto, "Creep and stress relaxation behavior for natural cellulose crystal of wood cell wall under uniaxial tensile stress in the fiber direction," *Journal of Wood Science*, vol. 64, no. 6, pp. 745–750, Dec. 2018, doi: 10.1007/s10086-018-1767-z.

[28] M. R. Asyraf, M. R. Ishak, S. M. Sapuan, N. Yidris, R. A. Ilyas, M. Rafidah, and M. R. Razman, "Evaluation of design and simulation of creep test rig for full-scale crossarm structure," *Advances in Civil Engineering*, vol. 2020, Art. no. 6980918, Oct. 2020, doi: 10.1155/2020/6980918.

[29] M. R. Asyraf, M. Rafidah, M. R. Ishak, S. M. Sapuan, N. Yidris, R. A. Ilyas, and M. R. Razman, "Integration of TRIZ, morphological chart and ANP method for development of FRP composite portable fire extinguisher," *Polymer*

Composites, vol. 41, no. 7, pp. 2917–2932, Jul. 2020, doi: 10.1002/pc.25587.

[30] N. H. M. Zulfli and W. S. Chow, "Flexural and morphological properties of epoxy/glass fibre/silane-treated organo-montmorillonite composites," *Journal of Physical Science*, vol. 21, no. 2, pp. 41–50, 2010.

[31] D. Guner, O. Golbasi, and H. Ozturk, "Generic creep behavior and creep modeling of an aged surface support liner under tension," *Journal of Rock Mechanics and Geotechnical Engineering*, vol. 14, no. 2, pp. 377–384, Apr. 2022, doi: 10.1016/j.jrmge.2021.12.004.

[32] M. Muralidharan, T. P. Sathishkumar, J. de-Prado-Gil, and R. Martínez-García, "Long-term environmental bending behaviors and service life prediction of Kevlar fiber mat epoxy composite," *Polymer Composites*, vol. 43, no. 4, pp. 2396–2407, Apr. 2022, doi: 10.1002/pc.26549.

[33] G. Carra and V. Carvelli, "Long-term bending performance and service life prediction of pultruded glass fibre reinforced polymer composites," *Composite Structures*, vol. 127, pp. 308–315, Sep. 2015, doi: 10.1016/j.compstruct.2015.03.049.